Microwave-induced dielectronic recombination above the classical ionization limit in a static field

C. M. Evans, E. S. Shuman, and T. F. Gallagher
Department of Physics, University of Virginia, Charlottesville, Virginia 22904-4714
(Received 25 November 2002; published 29 April 2003)

The presence of a static electric field substantially enhances the dielectronic recombination (DR) rate below the classical field ionization limit and suppresses DR entirely above it. The addition of a small microwave field polarized orthogonally to the static field leads to a substantial DR signal above the classical ionization limit. We have examined DR from a continuum of finite bandwidth in static fields from 0 to 130 V/cm and with 8–11 GHz microwave fields of amplitudes up to 5 V/cm. We attribute the microwave-induced DR above the classical limit to the transfer of atoms by the microwave field from autoionizing the $m=0$ Rydberg intermediate states to higher m states. Since higher m states are more stable against field ionization, these states are more likely to decay radiatively to stable bound Stark states, thereby completing DR. This m-changing process most likely occurs by resonantly driving the $\Delta n=0$, $\Delta m=1$ transitions of the autoionizing Rydberg-Stark states with the microwave field.

DOI: 10.1103/PhysRevA.67.043410 PACS number(s): 32.80.Rm, 32.60.+i, 34.80.Lx

I. INTRODUCTION

Dielectronic recombination (DR), the recombination of an ion and an electron via a doubly excited autoionizing state, is an important recombination pathway for energetic electrons in high-temperature plasmas [1,2]. Since the bulk of DR passes through the autoionizing Rydberg states, even very small external electric fields have a substantial effect on the DR rates [1–8]. These fields can be the quasistatic fields from the ions in the plasma, the rapidly varying fields from the electrons in a plasma, or the macroscopic fields that are deliberately applied in controlled experiments to probe DR rates. Irrespective of the source, a static or quasistatic electric field has two effects [2–8]. First, it lowers the ionization limit to the classical field ionization limit (which we term the classical limit), above which no DR occurs. Second, below the classical limit, the DR rate is greatly increased due to Stark mixing of the ℓ states. (We follow the usual convention that n, ℓ, and m are the principal, angular momentum, and azimuthal angular momentum quantum numbers of the Rydberg electron.) Although magnetic fields were long thought to be of little consequence, it has recently been shown that a magnetic field perpendicular to an electric field can further increase the DR rate by mixing the m states as well [9–12].

Here we report the observation of microwave-induced DR from a continuum of finite bandwidth [13] above the classical limit in a static electric field. Presumably the microwaves, which are polarized perpendicular to the static field, mix the autoionizing $m=0$ Rydberg states of the entrance channel with nearly degenerate higher m states, which are much more stable against field ionization [14,15]. These higher m states are, therefore, more likely to decay radiatively to bound Rydberg states, thereby completing DR. The underlying physics is similar to that described in the study of magnetic field effects on recombination from a continuum of finite bandwidth [12] and in recent reports of recombination in a static electric field induced by a perpendicularly polarized half cycle pulse [16,17]. An important aspect of microwave-induced DR above the classical limit is the size of the effect. In the presence of a small perpendicular microwave field, the DR signals above and below the classical limit can be comparable.

In the sections that follow, we present a simple physical picture to explain the microwave field enhancement of DR above the classical limit, relate DR from a continuum of finite bandwidth to true DR, describe our experimental approach, and present and discuss our results.

II. ORIGIN OF THE MICROWAVE ENHANCEMENT

The origin of the microwave enhancement of DR is best understood by starting with a brief discussion of field ionization. Classical field ionization occurs by passing of an electron over the saddle point in the combined Coulomb-Stark potential. For a binding energy W of $-1/2n^2$, it is easy to show that the required ionization field is $E_{dc}=1/16n^4$, or that the classical limit for ionization W_{CL} occurs at

$$W_{CL}=-2\sqrt{E_{dc}}. \tag{1}$$

We have used atomic units and shall continue to do so unless units are explicitly given. Equation (1) is written assuming that atoms are in a $m=0$ state, where the field direction coincides with the quantization axis. States of higher m require slightly higher fields for ionization [14,15], because in these states the electron is kept away from the saddle point on the quantization axis by the centrifugal barrier.

Let us focus for a moment on hydrogen. For extreme red $m=0$ hydrogen Stark states, in which the electron is localized near the saddle point, ionization occurs at the field given by Eq. (1). By a red or blue Stark state we mean one that is shifted to lower or higher energy, respectively, by the field. These extreme red Stark states are shifted down in energy by $-3n^2E_{dc}/2$ so, in terms of their principal quantum number, ionization occurs at the field $E_{dc}=1/9n^4$. In the blue-shifted hydrogenic Stark states the electron is localized on the side of the atom opposite the saddle point and kept away from the saddle point by a potential analogous to a centrifugal potential. As a result, the bluest state, for any given value of n,

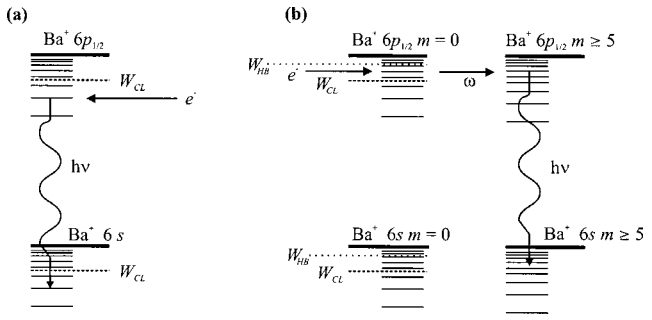

FIG. 1. (a) Schematic level diagram for DR in the presence of a static electric field. (b) Schematic level diagram for DR in the presence of crossed static and microwave fields. The bold solid lines represent the zero-field ionization limits. The broken lines represent the classical field ionization limit W_{CL}. The dotted lines represent the hydrogen blue state ionization limit W_{HB}.

requires the highest field for ionization. For the extreme blue $m=0$ Stark state, the required field for ionization is $E_{dc}=1/4n^4$, in spite of the fact that the Stark shift of the state is $+3n^2E_{dc}/2$. If we combine the energy of the bluest $m=0$ Stark state, namely, $W=-1/2n^2+3/2n^2E$, with the ionization field $E_{dc}=1/4n^4$, we obtain the classical ionization limit for the bluest hydrogenic states. Explicitly,

$$W_{HB}=-\tfrac{1}{4}\sqrt{E_{dc}}. \tag{2}$$

Thus, in hydrogen, there are no classically unstable states below W_{CL} [i.e., Eq. (1)], and there are no stable ones above W_{HB} [i.e., Eq. (2)]. Stark states between the reddest and bluest states ionize at fields between $1/9n^4$ and $1/4n^4$. Since the bluer states have higher energies but ionize at higher fields, there are necessarily stable blue states that are degenerate with ionizing red states of higher n. However, these states are not coupled to each other, implying that stable blue states can exist above W_{CL}.

In Ba, or in any non-hydrogenic atom, the finite-sized ionic core couples the red and blue Stark states of different n. The degree of coupling is proportional to the quantum defects of the zero field ℓ states of a given m. For $m=0$ states, all the quantum defects play a role; while for $m=5$ states, only those of $\ell\geqslant 5$ are important. For low-m Ba states above the classical limit, W_{CL}, ionization of states other than the reddest states occurs by core coupling into the rapidly ionizing degenerate red states of higher n [18]. For high-m Stark states of Ba, those with near-zero quantum defects, the core coupling is so small as to be negligible. Thus, high-m states in the nonhydrogenic atoms such as Ba behave similarly to hydrogen, that is, substantially higher fields are required for ionization in comparison to low-m Ba states.

After this brief discussion of field ionization it is easy to understand the profound effect of a microwave field polarized orthogonally to a static electric field. In Fig. 1(a), we schematically depict DR in the presence of a static electric field with no microwaves. The classical limits of Eq. (1), W_{CL}, below the Ba^+ $6p_{1/2}$ and $6s_{1/2}$ limits are shown as broken lines. As illustrated, an electron incident on a Ba^+ $6s_{1/2}$ ion with an energy below the $6p_{1/2}$ classical limit can be captured into a stable $6p_{1/2}$ Stark state, and then radiative decay to the analogous stable $6s_{1/2}$ Stark state to complete DR. An incident electron with an energy above the $6p_{1/2}$ classical limit ionizes from the very unstable $6p_{1/2}$ Stark states before radiative decay to stable $6s_{1/2}$ Stark states, and therefore DR can occur.

When the perpendicular microwave field is present, it allows the additional process shown in Fig. 1(b) to occur. An electron initially captured into an unstable $m=0$ Stark state above the classical limit W_{CL} is transferred to a higher m state by the microwave field. Below the classical limit for hydrogenic blue states, W_{HB}, shown by the dotted line, there are stable hydrogen-like high-m states that can radiate to bound $6s$ Stark states, thus completing DR. Note that the microwave field must be turned off immediately after the laser pulse, otherwise atoms in high-m states will return to low-m states and field ionize. In summary, the microwave field transfers the atoms from unstable nonhydrogenic $m=0$ states to stable hydrogenlike states of high m (i.e., $m\geqslant 4$).

III. DIELECTRONIC RECOMBINATION FROM A CONTINUUM OF FINITE BANDWIDTH

True DR in Ba is a recombination of a free electron with a ground state Ba^+ $6s_{1/2}$ ion, as shown in Fig. 1. In DR from a continuum of finite bandwidth, the free continuum electron is replaced by one from the continuum of finite bandwidth, namely, the 100 cm^{-1} wide $6p_{3/2}$ $11d$ state, which straddles the $6p_{1/2}$ limit. In addition, the initial state of the Ba^+ ion is $6p_{3/2}$. In zero field the two processes may be written as

$$Ba^+\ \ 6s_{1/2}+e^-\rightarrow Ba\ \ 6p_{1/2}n\ell\rightarrow Ba\ \ 6s_{1/2}n\ell+h\nu \tag{3}$$

for true DR, and

$$Ba\ \ 6p_{3/2}11d\rightarrow Ba\ \ 6p_{1/2}nd\rightarrow Ba\ \ 6s_{1/2}nd+h\nu \tag{4}$$

for DR from a continuum of finite bandwidth.

The differences between the processes of Eqs. (3) and (4) are that the $11d$ electron is not truly free; it circulates about the Ba^+ core for roughly 20 orbits before autoionization. Thus, the $11d$ orbit is, in effect, a small storage ring. Furthermore, the ionic transition is a quadrupole transition, not a dipole transition; however, this difference is of little consequence in electron scattering. The advantage of using the continuum of finite bandwidth to study DR is that, unlike traditional storage ring experiments, zero electric and magnetic field studies are possible.

IV. EXPERIMENTAL APPROACH

Ba atoms in an atomic beam are excited to the continuum of finite bandwidth, the Ba $6p_{3/2}11d$ state, by three 5 ns dye lasers (cf. Fig. 2). The first two lasers are fixed in energy to drive the transitions $6s^2\rightarrow 6s6p$ and $6s6p\rightarrow 6s11d$. The third laser, which drives the $6s11d\rightarrow 6p_{3/2}11d$ transition, is scanned in frequency near the Ba^+ $6p_{1/2}$ limit. The excita-

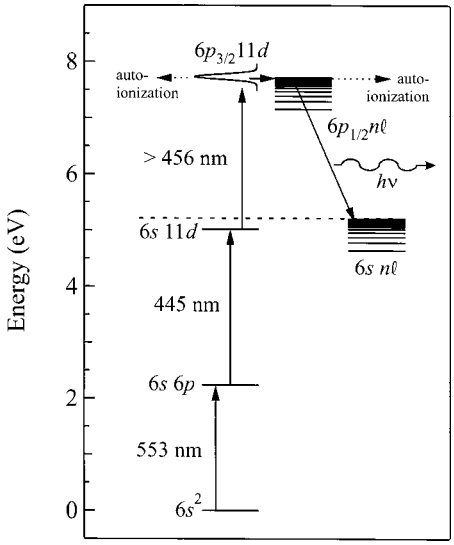

FIG. 2. Barium energy level diagram for dielectronic recombination from a continuum of finite bandwidth. Three dye lasers are used to drive the transitions from the Ba $6s^2$ ground state to the $6p_{3/2}11d$ state, which is the continuum of finite bandwidth. From it, the $11d$ electron can either autoionize into the true continuum (represented by the horizontal dotted lines) or be captured into degenerate $6p_{1/2}n\ell$ states (represented by the horizontal solid line). If capture occurs, the $6p_{1/2}n\ell$ state can either autoionize or decay radiatively down to a stable $6sn\ell$ state. In the latter case, dielectronic recombination has occurred and is detected by field ionization of the $6sn\ell$ Rydberg states.

tion occurs in the presence of a static electric field and a microwave field, which is typically switched off 3 ns after the third dye laser pulse. A field ionization pulse of 380 V/cm is applied 3.5 μs after the third laser pulse to ionize atoms, which DR has left in high lying, bound Ba $6snd$ or $6snk$ Rydberg states. We detect the electrons from these atoms as the frequency of the third laser is scanned.

The geometry of the interaction region is shown in Fig. 3. The Ba atomic beam passes down the axis of a set of four

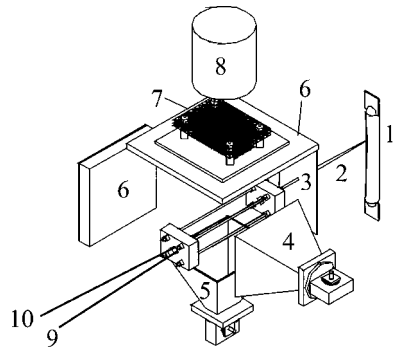

FIG. 3. Schematic diagram of the experimental apparatus showing (1) the oven, (2) the atomic beam, (3) the collimator, (4) the microwave horn for parallel field experiments, (5) the microwave horn for perpendicular field experiments, (6) the microwave absorbers, (7) the mesh, (8) the microchannel plate detector, (9) the collinear first and second dye laser beams, and (10) the third dye laser beam.

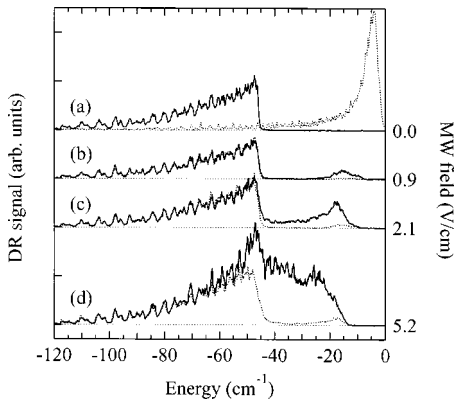

FIG. 4. Dielectronic recombination signals as observed when scanning the third laser of Fig. 2. (a) DR with no microwave field. (· · · · ·) no static electric field and (—) 56 V/cm static electric field. (b)–(d) DR with a 8.0-GHz microwave fields from 0 to 5.2 V/cm in (· · · · ·) parallel fields and (—) perpendicular fields. The traces are offset in intensity by the microwave field. All data are intensity normalized in the same spectral region. The energy is relative to the zero-field $6p_{1/2}$ ionization limit.

parallel rods 0.24 cm in diameter and 1.9 cm apart. The static and pulsed electric fields are vertical, and the laser beams are all polarized vertically so as to excite $m=0$ states, although we did not see any significant difference with other laser polarizations. The intersection of the laser beams with the atomic beam defines the interaction region. As depicted in Fig. 3, there are microwave horns below and to the side of the interaction region that allow the application of microwave fields parallel and perpendicular to the static electric field. Based on the mechanical precision of this arrangement and the variation in direction of the static field over the interaction volume, we estimate that the static and microwave fields are parallel and perpendicular to within 5°.

The microwave source is a Hewlett-Packard (HP) 8685B oscillator, which produces 10 mW of output at 5–12 GHz. The output of the oscillator is formed into pulses, using an ARRA high-speed microwave switch with a rise and fall time of 5 ns. The microwave pulses are then amplified to 6 W and sent to one of the two microwaves horns. The 8.0 and 11 GHz microwave field amplitudes were calibrated by comparing the effect of the microwave field on the DR signal in zero static field to similar data published previously [19–21]. The maximum 8.0 GHz microwave field that we can produce is 5 V/cm and the maximum 11.0 GHz microwave field is 4 V/cm. The uncertainty in the microwave field is ±25%.

V. OBSERVATIONS

In Fig. 4 we show typical scans of the third laser frequency under several conditions. In Fig. 4(a) we present the DR signals obtained with no static field (dotted line) and with a static electric field E_{dc} of 56 V/cm and no microwave field (solid line). Above $W_{CL}=-45.81\ \mathrm{cm}^{-1}$, the classical ionization limit, we see no DR in the 56 V/cm trace and, below W_{CL}, there is a substantial increase in the DR signal in comparison to the signal in the absence of E_{dc}. This increase is due to the Stark mixing of ℓ states by the static

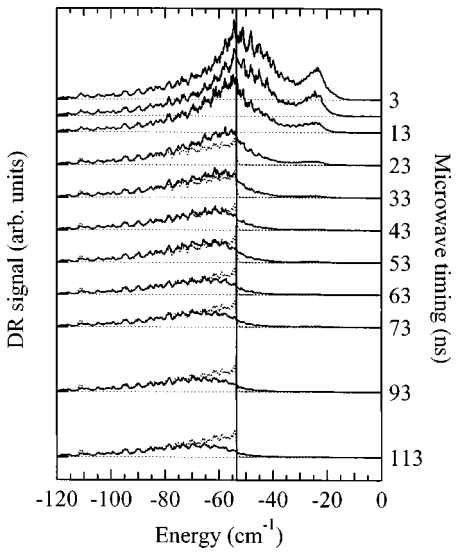

FIG. 5. Dielectronic recombination signals observed with different lengths of microwave pulse obtained by scanning the third laser of Fig. 2. There is a 5.2-V/cm, 8.0-GHz microwave field perpendicular to a 75.5-V/cm static electric field. The traces are offset by the time delay between the third laser pulse and when the microwaves are turned off. Different traces are intensity normalized in the energy region, $-120\ \mathrm{cm}^{-1} < W < -100\ \mathrm{cm}^{-1}$. (·····) is the DR signal without the microwave field and (—) is the DR signal in the presence of the microwave field. The thick solid line is the classical field ionization limit. The energy is relative to the zero-field $6p_{1/2}$ ionization limit.

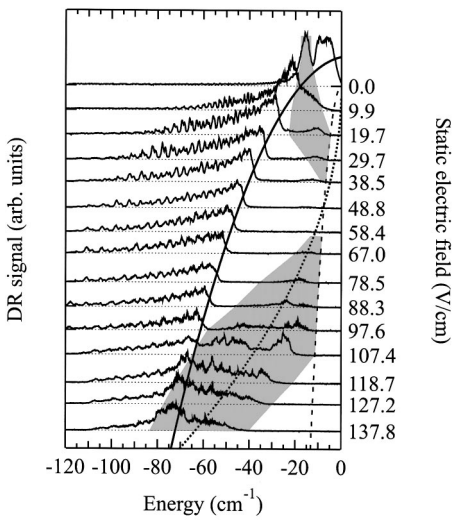

FIG. 6. Dielectronic recombination signals as observed when scanning the third laser of Fig. 2 in a 4.1-V/cm, 11.0-GHz microwave field perpendicular to a sequence of static electric fields. The data are offset by the static electric field and are intensity normalized in the energy, $-120\ \mathrm{cm}^{-1} < W < -100\ \mathrm{cm}^{-1}$, for static fields down to 38.5 V/cm. At lower static fields higher energy ranges were used. The thick solid line is the classical field ionization limit W_{LC} [i.e., Eq. (1)]. The broken line is the classical ionization limit for the blue-most hydrogen Stark states, W_{HB} [i.e., Eq. (2)]. The dotted line corresponds to Eq. (6). The gray shaded area in the upper part of the graph corresponds to the stable Stark states that undergo the $\omega = 1/n^3$ resonant transition. The gray shaded area in the lower part of the graph corresponds to the stable Stark states that undergo the $\omega = 3nE/2$ resonant transition. The energy is relative to the zero-field $6p_{1/2}$ ionization limit.

electric field. As illustrated by Fig. 4(b) which depicts the DR signal at $E_{dc} = 56$ V/cm with an 8.0-GHz microwave field of 0.9 V/cm, we see a clear DR signal above the classical limit if the microwave field is polarized perpendicular to the static electric field (solid line), but a barely visible signal with the microwaves polarized parallel to the static field (dotted line). In an 8.0-GHz, 2.1-V/cm microwave field [cf. Fig. 4(c)] the DR signal with perpendicular polarization (solid line) fills in the gap between the peak of Fig. 4(b) and the classical limit W_{CL}. Moreover, the peak 50 cm^{-1} above the classical limit is now clearly visible with parallel polarization (dotted line). At the higher microwave field of 5.2 V/cm [cf. Fig. 4(d)] the classical limit is no longer obvious with a perpendicular microwave field (solid line), and the DR signal above the classical limit now covers a broader energy range with parallel polarization (dotted line).

As mentioned earlier, we usually turn off the microwaves with a 3-ns delay after the third laser pulse, for most of the DR signal disappears quickly with increasing time delay. The decrease of the signal with time delay is shown explicitly in Fig. 5, obtained with a static field of 75.5 V/cm and a 5.2-V/cm, 8.0-GHz microwave field. Two points are evident in Fig. 5. First, the peak at an energy of -25 cm^{-1}, 30 cm^{-1} above the classical limit of -53.19 cm^{-1} disappears very quickly. Second, as the energy above the classical limit is increased, the DR signal decays more rapidly. Only the DR signals just above the classical limit persist for a 100-ns delay in turning off the microwave field.

As described in Sec. II the origin of the above threshold DR signals shown in Figs. 4 and 5 is that the microwaves mix relatively unstable $m = 0$, $6p_{1/2}nk$ Stark states, which are the entrance channel from the $6p_{3/2}11d$ state, with more stable, high-m $6p_{1/2}nk$ Stark states. These high-m states are more likely to radiate to bound $6snk$ states than to field ionize. To demonstrate that the origin is not decay from a rapidly ionizing $6p_{1/2}nk$ state to a rapidly ionizing $6snk$ Stark state followed by a transition to a stable state, we have directly excited the $6snk$ states above the classical limit, with the second laser, in the presence of a microwave field. In these experiments, the timing of the microwaves was identical to the timing during the study of DR. Only just above the classical limit in *dc* fields greater than 50 V/cm can we observe a signal, which is comparable to the long-time delay signals of Fig. 5.

In Fig. 6 we present the DR signals observed in a range of static fields with an 11-GHz microwave field. Similar data were taken at 8.0 GHz and are not shown for brevity. These data show two interesting features. First, we note that the DR signal never extends above W_{HB}, the highest energy at which we expect to find a blue, hydrogenic Stark state (cf. Fig. 6, dashed line). Second, in Sec. II we suggested that the mechanism for the microwave enhancement above the classical limit is transitions from the initial $m = 0$ states to higher-m states. Evidence for the resonant nature of these

microwave transitions can be seen in Fig. 6. In fact, there are two different resonances.

At zero field the expected enhancement at the $\Delta n=1$ resonance [19–21],

$$\omega = 1/n^3, \tag{5}$$

which occurs at $W=-15.51\ \mathrm{cm}^{-1}$, is quite apparent. This resonance persists above the classical limit and well beyond the Inglis-Teller limit, where the Stark states of adjacent n overlap. In spite of the large Stark shifts, the resonance frequency is almost unchanged from $\omega=n^{-3}$ because there exists a strong propensity for $\Delta n=1$ transitions between Stark states with similar Stark shifts [14,22].

An estimate of the range of n over which the $\Delta n=1$ resonance occurs can be obtained by comparing the Rabi frequency for the transition to the detuning. The $\Delta n=1$ Rabi frequency is given approximately by $\Omega=0.3n^2\ E_{mw}/2$. The factor of 2 in the field comes from the rotating wave approximation. Thus, for $n=85$, the location of the 11.0 GHz, $\Delta n=1$ resonance, $\Omega=1.3$ GHz at $E_{mw}=1$ V/cm. The $\Delta m=1$ transition probability for a long microwave pulse is $T=\Omega^2/(\Omega^2+\Delta^2)$, where Δ is the detuning of the microwave frequency from the $\Delta n=1$ interval. To stabilize the atoms that initially have $m=0$, we expect to drive them to the hydrogenic $m\geqslant 5$ states. A reasonable estimate for the $\Delta m=5$ transition probability is given by $T=[\Omega^2/(\Omega^2+\Delta^2)]^5$. The half maximum for this expression occurs at $\Delta=0.4\Omega=2$ GHz, at $E_{mw}=4$ V/cm, which implies that the $\Delta n=1$ resonance condition is fulfilled for $n=85\pm 6$ for $E_{mw}=4$ V/cm. This model predicts the breadth of the zero-field resonance to be 4 cm^{-1}, in reasonable agreement with our observations. In an electric field far larger effects are the energy spreading of the $m=0$ Stark states of a given n, $\Delta W=\pm 3n^2E_{dc}/2$ [14], and the field ionization of the Stark states. The spreading of the stable hydrogenic Stark states is shown by the gray area on the top six traces of Fig. 6. It is clear that the observed $\Delta n=1$ resonance falls mostly within the band defined by this area. Another interesting feature is that the resonance shifts to slightly higher energy, and is obviously cut off at W_{HB}. The shift to higher energy occurs because the resonance condition requires $n\sim 85$, and for $E_{dc}>10$ V/cm only the bluest hydrogen-like $n=85$ states are stable.

At the fields above 50 V/cm, as the $\Delta n=1$ resonance disappears, a new feature begins to emerge, which we attribute to the $\Delta m=1$ resonance between the adjacent hydrogenic Stark levels of the same n. In the linear Stark effect this resonance should occur at

$$\omega = 3nE_{dc}/2, \tag{6}$$

which is shown by the dotted line in Fig. 6. The energy range over which this resonance appears is determined by the range of n over which the coupling is resonant, the Stark shifts of these levels, and whether or not the levels are stable against field ionization. To calculate the range of n over which this resonance can be driven by the microwave field, we need the matrix elements for the $\Delta m=1$ transitions. At the center of the Stark manifold the matrix element coupling an $m=0$ level to the nearby $m=1$ level is $0.75n^2$, while at the edge of the manifold it falls to $0.5n^2$. At the edge of the manifold the Rabi frequency is thus $\Omega=0.5n^2(E_{m\omega}/2)$. Assuming again that five $\Delta m=1$ transitions are required, we conclude that the half point of the transition probability occurs for $\Delta=0.4\Omega$. For an 11-GHz microwave field and a static field of 138 V/cm, Eq. (6) is satisfied for $n=42$. For a microwave field amplitude of 4 V/cm, we calculate a Rabi frequency of 2.2 GHz, which implies that the states of $n=42\pm 3$ should be resonant with the microwave field. In zero field this band of states covers 22 cm^{-1}, which is smaller than the energy spreading of each Stark manifold, $3n^2E_{dc}$, which is 32 cm^{-1} at $n=42$. Thus, the width of the band of states, which contribute to the microwave enhancement, is determined by the edges of the Stark manifolds. It is for this reason that we used $0.5n^2$ as the matrix element to calculate the Rabi frequency.

As we lower the static field, raising the value of n at which the $\Delta n=0$, $\Delta m=1$ resonance occurs, the band of states should become wider due to the n^2 dependence of the $\Delta n=0$, $\Delta m=1$ matrix element. However, with a microwave field of 4 V/cm, at the center of the $n=75$ Stark manifold the Rabi frequency$=11$ GHz, and this model is unlikely to work. Accordingly, we have assumed that the number of resonant n states increases linearly with n from $n=42\pm 3$ at 137.8 V/cm to $n=85\pm 22$ at 67.0 V/cm, as this assumption fits the data. In Fig. 6 the lower gray band shows the states that should contribute to the $\Delta n=0$, $\Delta m=1$ resonance of Eq. (6). At high static field, or low n, it simply reflects the extent of the Stark manifolds of the n states that are resonant, and it is nearly symmetric about the dotted line representing Eq. (6). At lower field and higher n the band is cut off on the high-energy side by W_{HB} and on the low-energy side by the field ionization of the red Stark states that are hydrogenically unstable. To take the field ionization into account we assume that the red states ionize at $E=1/9n^4$ and the blue states at $E=1/4n^4$, and that the ionization fields of intermediate states are obtained by interpolating between these two values. Those states, which are hydrogenically unstable, do not contribute.

In Fig. 7(a), we present the difference between the DR signals in crossed static and microwave fields (cf. Fig. 6) and the DR signals in the absence of the microwave field for $E_{dc}>70$ V/cm. To make a comparison of these data with the explanation presented above, we have calculated the density of stable hydrogenic $m=0$ states that are resonant. This calculation is essentially the same as that carried out to calculate the lower gray area of Fig. 6; however, it differs in that in which we have also taken into account the fact that the $\Delta n=0$, $\Delta m=1$ matrix element falls from $0.75n^2$ at the center of the manifold to $0.5n^2$ at the edge of the manifold, which modifies the intensity of the various states contributing to any given point in the calculated spectrum. In calculating the Stark shift, we have included terms up to third order, which shift all states to lower energy. The resulting density of resonant states is shown in Fig. 7(b), which does indeed look qualitatively similar to Fig. 7(a).

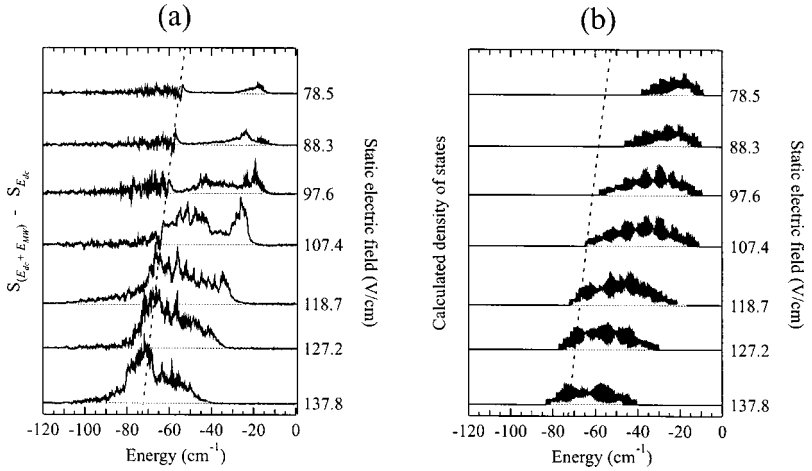

FIG. 7. (a) The difference between the DR signal in perpendicular fields $S_{(E_{dc}+E_{MW})}$ of Fig. 6 and the DR signal without the microwave field $S_{E_{dc}}$ for $E_{dc}>70$ V/cm. (b) Calculated density of resonant states. See text for discussion. The energy is relative to the zero field $6p_{1/2}$ ionization limit.

Finally, it is useful to compare the Rabi frequencies to the lifetimes of the initial Ba $m=0$ states against field ionization, the point being that the microwaves must transfer the $m=0$ atom to higher m before field ionization if DR is to occur. As in Sec. II, in the energy range $W_{CL}<W<W_{HB}$, Ba states field ionize by core scattering of the electron, which takes atoms from Stark states other than the red-most state to unstable red states of higher n. As a crude approximation, we assume that this scattering-induced field ionization occurs at the same ionization rate as Ba $6p_{1/2}nk$ autoionization rates in a field, that is, we assume that the $m=0$ states have a field ionization rate [23]

$$\Gamma_{FI}=0.53n^{-4}, \tag{7}$$

which gives a rate of ~1 GHz at $n=43$, the lowest n we observed. Thus, it appears that $\Omega>\Gamma_{Fl}$ when we observe the microwave enhancement, which is certainly a necessary condition.

When examined in detail, the isolated structures observed above the classical limit can be quite striking, as shown by Fig. 8(a). We interpret this structure as arising from the density of $m=0$ Stark states. Figure 9 is a plot of the calculated hydrogenic $m=0$ energy levels near $W=-15$ cm^{-1} in field around 82 V/cm, using a hydrogenic calculation. At fields near the Inglis-Teller field, $E=1/3n^5$, using a hydrogenic model to calculate Ba $m=0$ energies, would give meaningless results due to the large avoided level crossings between red and blue Stark states of different n [24,25]. However, at the fields shown in Fig. 9 the red states, the major source of the differences between hydrogen and Ba are absent. Recent measurements of the Stark structure of Ba in this field-energy regime show hydrogen-like energy levels [26]. As shown in Fig. 9(a) for energies above $W=-10$ cm^{-1} there are no stable levels, since the energy is above W_{HB}. The highest stable levels are at $W\approx-10$ cm^{-1}, and for $E_{dc}<81$ V/cm they are the $n=63$ levels and for $E_{dc}\geqslant 81$ V/cm they are the $n=62$ levels. Note that at $E=81.5$ V/cm, the field of Fig. 8(a), there are superimposed levels of different n. The Stark levels of different n are superimposed if the zero-field Δn spacing is an integral multiple of the spacing between the $m=0$ Stark levels of the same n, i.e., if

$$3nEj=\frac{1}{n^3}, \tag{8}$$

where j is an integer. Inspecting Fig. 9 we can see that $j=2$. For a field of 81 V/cm and $j=2$ this condition is satisfied for $n=57$, in a reasonable agreement with the result shown in Fig. 9 for the higher-order calculation. As the energy is decreased the Stark levels of different n should be superimposed when Eq. (8) is satisfied for higher values of j, and a plot of the energy levels resembles a Moire pattern, as shown in Fig. 9.

While Fig. 9 provides a graphical explanation of the origin of the well-defined structure evident in Fig. 8(a), it does not allow quantitative comparison to the observed spectra. To make such a comparison, we use the method discussed above to calculate the density of states for $E_{dc}=81.5$ V/cm for all stable Stark states in the energy range shown in Fig. 9. Not

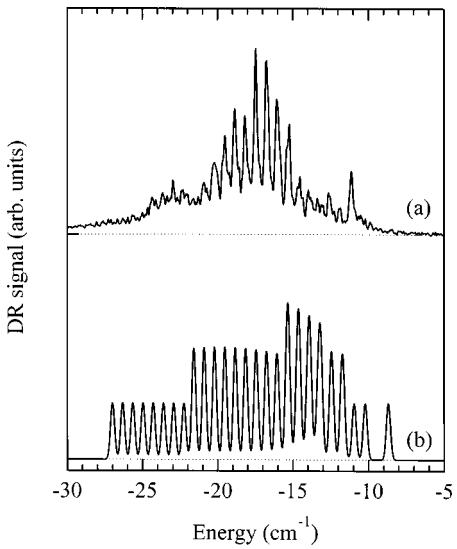

FIG. 8. (a) Dielectronic recombination signal observed when scanning the third laser of Fig. 1 in a 81.5-V/cm static electric field with a 0.5-V/cm perpendicularly polarized microwave field of 11 GHz. (b) Synthetic dielectronic recombination spectra calculated in a 81.5-V/cm static field with a microwave frequency of 11 GHz. The energy is relative to the zero-field $6p_{1/2}$ ionization limit.

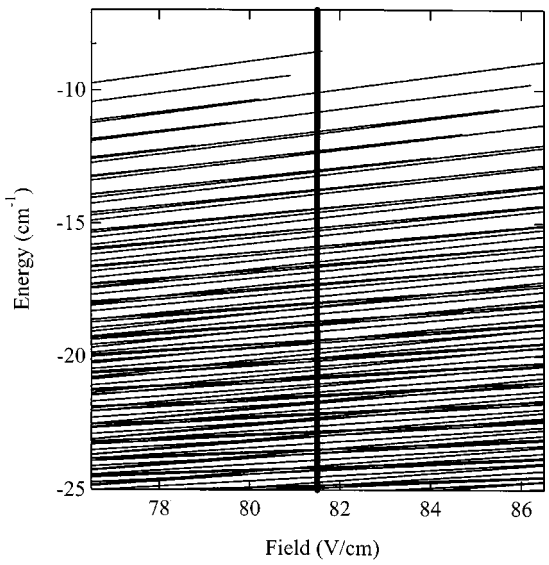

FIG. 9. The hydrogenic Stark map of stable blue states around the binding energy $W=-15\,\mathrm{cm}^{-1}$ and the static electric field of 81.5 V/cm. Note the areas along the thick vertical line where the levels are essentially superimposed.

all of the states satisfy the resonance condition of Eq. (6) for the 11-GHz microwave frequency. Accordingly, we select only those states that are within the resonance band for the $\Delta n=0$, $\Delta m=1$ transition at 11 GHz. This selection corresponds to the lower gray area of Fig. 6. The resulting density of states is convoluted with the laser linewidth to give the synthetic spectrum shown in Fig. 8(b). Comparison of Fig. 8(b) to the experimental spectra of Fig. 8(a) shows that they are quite similar.

VI. CONCLUSION

The presence of a static electric field raises the DR rate dramatically below the classical limit W_{CL}, but eliminates it above W_{CL}. Adding a microwave field polarized perpendicular to the static field makes DR above the classical limit possible, at times with a rate comparable to the rate below the limit. The above threshold becomes possible because the microwave field mixes the $m=0$ states, which are the entrance channel for DR and have rapid, nonhydrogenic field ionization rates, with high-m states that have slower, hydrogenic field ionization rates. These observations imply that in a true plasma, in which ions provide a quasistatic field and the electrons provide a randomly oriented time varying field, DR can still occur above the classical limit imposed by the ion microfields, raising the DR rate above what would be expected on the basis of the classical limit. Similarly, in controlled measurements of DR rates in merged beams or storage rings, the incoming electrons can be in any ℓ state (not $\ell=2$ as we have here). To an extent that high-ℓ, nearly hydrogenic, states are important [27]; our measurements suggest that there might be substantial DR above the classical limit in these well-controlled experiments as well.

ACKNOWLEDGMENTS

It is a pleasure to acknowledge useful conversations with R. R. Jones and the support of Basic Energy Sciences of the U.S. Department of Energy.

[1] A. Burgess, Astrophys. J. **139**, 776 (1964).
[2] A. Burgess and H. P. Summers, Astrophys. J. **157**, 1009 (1969).
[3] V. L. Jacobs, J. Davis, and P. C. Kepple, Phys. Rev. Lett. **37**, 1390 (1976).
[4] A. Müller, D. S. Belić, B. D. DePaola, N. Djurić, G. H. Dunn, D. W. Mueller, and C. Timmer, Phys. Rev. A **36**, 599 (1987).
[5] P. F. Dittner, S. Datz, R. Hippler, H. F. Krause, P. D. Miller, P. L. Pepmiller, C. M. Fou, Y. Hahn, and I. Nasser, Phys. Rev. A **38**, 2762 (1988).
[6] T. Bartsch, A. Müller, W. Spies, J. Linkemann, H. Danared, D. R. DeWitt, H. Gao, Z. Wong, R. Schuch, A. Wolf, G. H. Dunn, M. S. Pindzola, and D. C. Griffin, Phys. Rev. Lett. **79**, 2233 (1997).
[7] J. G. Story, B. J. Lyons, and T. F. Gallagher, Phys. Rev. A **51**, 2156 (1995).
[8] L. Ko, V. Klimenko, and T. F. Gallagher, Phys. Rev. A **59**, 2126 (1999).
[9] F. Robicheaux and M. S. Pindzola, Phys. Rev. Lett. **79**, 2237 (1997).
[10] K. LaGattuta and B. Borca, J. Phys. B **31**, 4781 (1998).
[11] T. Bartsch, S. Schippers, A. Müller, C. Brandau, G. Gwinner, A. Saghiri, M. Beutelspacher, M. Grieser, D. Schwalm, A. Wolf, H. Danared, and G. H. Dunn, Phys. Rev. Lett. **82**, 3779 (1999).
[12] V. Klimenko, L. Ko, and T. F. Gallagher, Phys. Rev. Lett. **83**, 3808 (1999).
[13] J. P. Connerade, Proc. R. Soc. London, Ser. A **362**, 361 (1978).
[14] H. A. Bethe and E. E. Salpeter, *Quantum Mechanics of One and Two Electron Atoms* (Academic Press, New York, 1957).
[15] T. F. Gallagher, *Rydberg Atoms* (Cambridge University Press, Cambridge, 1994).
[16] J. G. Zeibel and R. R. Jones, Phys. Rev. Lett. **89**, 093204 (2002).
[17] J. G. Zeibel, S. N. Pisharody, and R. R. Jones (unpublished).
[18] M. G. Littman, M. M. Kash, and D. Kleppner, Phys. Rev. Lett. **41**, 103 (1978).
[19] V. Klimenko and T. F. Gallagher, Phys. Rev. Lett. **85**, 3357 (2000).
[20] V. Klimenko and T. F. Gallagher, Phys. Rev. A **66**, 023401 (2002).
[21] V. Klimenko, Ph.D. thesis, University of Virginia, 2002 (unpublished).
[22] E. Murgu, J. D. D. Martin, and T. F. Gallagher, J. Chem. Phys. **115**, 7032 (2001).
[23] R. R. Jones and T. F. Gallagher, Phys. Rev. A **39**, 4583 (1989).
[24] M. L. Zimmerman, M. G. Littman, M. M. Kash, and D. Kleppner, Phys. Rev. A **20**, 2251 (1979).

[25] M. L. Zimmerman, T. W. Ducas, M. G. Littman, and D. Kleppner, J. Phys. B **11**, L11 (1978).
[26] R. R. Jones (private communication).
[27] C. Brandau, T. Bartsch, A. Hoffknecht, H. Knopp, S. Schippers, W. Shi, A. Muller, N. Grun, W. Scheid, T. Steih, F. Bosch, B. Franzke, C. Kozhubarov, P. H. Mokler, F. Nolden, M. Steck, T. Stohiker, and Z. Stachura, Phys. Rev. Lett. **89**, 053201 (2002).